文章编号：1001-9014(XXXX)XX-0001-09

DOI:10.11972/j.issn.1001-9014.XXXX.XX.001

# Design of a wideband non-uniform microstrip line for complex impedance matching in automotive radar frequencies

ZHANG Shuang-Gen[1], YU Tao[1], WANG Yu-Lan[1], CHENG Zhi-Hua[1,2*], YAO Jian-Quan[2]

(1. Tianjin Key Laboratory of Film Electronic and Communication Devices, School of Integrated Circuit Science and Engineering, Tianjin University of Technology, Tianjin 300384, China;
2. The Institute of Laser & Opto-electronics, Tianjin University, Tianjin 300191, China)

**Abstract**: Microstrip transmission lines connecting to the millimeter wave radar chip and antenna significantly affect the radiation efficiency and bandwidth of the antenna. Here, a wideband non-uniform wavy microstrip line for complex impedance in automotive radar frequency range is proposed. Unlike the gradient transmission line, the wavy structure is composed of periodically semi-circular segments. By adjusting the radius of the semi-circular, the surface current is varied and concentrated on the semi-circular segments, allowing a wider tunability range of the resonant frequency. The results reveal that the bandwidth of the loaded wavy transmission line antenna improves to 9.37 GHz, which is 5.81 GHz wider than that of the loaded gradient line. The gain and the half power beam width of the loaded antenna are about 14.69 dB and 9.58°, respectively. The proposed non-uniform microstrip line scheme may open up a route for realizing wideband millimeter-wave automotive radar applications.

**Key words**: millimeter wave, gradient line, wavy transmission line, broadband, high gain array antenna

# 适用于汽车毫米波雷达频率复杂阻抗匹配的宽带非均匀微带线设计

张双根[1]，于 涛[1]，王玉兰[1]，程志华[1,2*]，姚建铨[2]

(1. 天津理工大学 集成电路科学与工程学院 天津市薄膜电子与通信器件重点实验室，天津 300384；
2. 天津大学 激光与光电研究所，天津 300191)

**摘要**：连接毫米波雷达芯片和天线的微带传输线对天线的辐射效率和带宽有重要影响。本文提出了一种适用于汽车雷达频率范围内复杂阻抗匹配的宽带非均匀微带线。与渐变传输线不同，波浪形传输线由周期性的半圆短段组成。通过调整半圆的半径，表面电流产生变化并且集中在半圆部分，从而获得更宽的谐振频率可调范围。结果表明，加载波浪线毫米波雷达天线的带宽提高到9.37 GHz，比加载渐变线宽5.81 GHz。加载波浪传输线后天线的增益为14.69 dB，半功率波束宽度约为9.58°。本文提出的非均匀微带线方案为实现毫米波雷达扩展宽带的应用提供了重要的思路。

**关 键 词**：毫米波；渐变线；波浪传输线；宽带；高增益阵列天线

**中图分类号**：O441.4　　**文献标识码**：A

## Introduction

Millimeter wave radar is widely used in unmanned driving, smart homes and health detection due to its all-weather operation, high precision and easy miniaturization[1,2]. Compared with substrate integrated waveguide (SIW) antennas[3], microstrip transmission line antennas are favored owing to their low profile, light weight, and ease of integrated manufacturing[4,5]. Meanwhile, they face the problem of narrow impedance bandwidth resulting from high loss[6]. The feed network has been designed to adjust the feed of the radiation patch in parallel arrays with high gain and wide bandwidth[7]. However, the complex feed transmission network increases the en-

**Received date**: 2024-09-10, **revised date**: 2024-11-16　　**收稿日期**：2024-09-10，**修回日期**：2024-11-16

**Foundation items**: Supported by the National Natural Science Foundation of China (61974104)

**Biography**: Zhang Shuang-Gen (1979-), male, Anhui, China, professor. Research interests include microwave photonic signal processing, micro-nano photonic devices and applications, and signal modulation recognition. Email: shgzhang@tjut.edu.cn

*Corresponding author: E-mail: asakaka1982@163.com

ergy loss and antenna size. The traditional quarter-impedance microstrip transmission line provides a limited impedance bandwidth for millimeter-wave radar antennas, with the bandwidths of 1.7 GHz[8] and 2 GHz[9]. To extend the bandwidth of millimeter-wave radar antennas, researchers have presented a method of incorporating a stepped transmission line structure based on the quarter impedance matching[10]. The antenna is equipped with periodically inverted trapezoidal angles to match with the stepped structure of the transmission line. Although the method yields a broadband, it has a low gain. Furthermore, the stepped transmission line leads to an increased antenna size with the gradual increase in transmission line order, which is not conducive to space-saving on the plate. More recently, an inverted conical millimeter-wave radar transmission line antenna with a bandwidth of only 1.3 GHz is investigated[11]. The curved transmission line has demonstrated to achieve a bandwidth of 8 GHz, yet it is actually not easy to fabricate due to its complex structure[12]. By adding radiation patches with various shapes coupled with the transmission line, multiple resonances at different frequencies can be generated. Although this type of comb radar transmission line antenna can obtain a wide impedance bandwidth, its radiation directivity is susceptible to significant changes[13-16]. The existing methods still face challenges from limited bandwidth, intricate structure and radiation efficiency.

In this paper, we propose a microstrip transmission line with non-uniform wavy impedance distribution for millimeter wave radar to achieve wide bandwidth. The wavy transmission line consists of microstrip and periodically semi-circular segments. By varying the semi-circular radius and the microstrip width, the surface current is concentrated on the semi-circular segments, resulting in a wider range of multiple resonant points matching. Compared to the tapered line, the non-uniform wavy microstrip transmission line significantly extends the antenna bandwidth, addressing the narrow-bandwidth issue in millimeter-wave automotive radar.

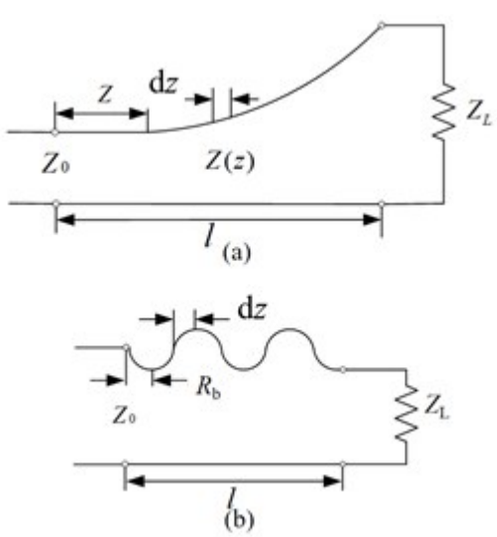


Fig. 1 Transmission line equivalent model
图1 传输线等效模型

## 1 Theoretical description of transmission line

Suppose that the length of the gradient line and the wave line are $l$, the characteristic impedance of the transmission line at the input end is $Z_0$, and the characteristic impedance of the transmission line at the output end is the load impedance $Z_L$, and $Z_L > Z_0$, as shown in Fig. 1.

The graded transmission line and the wavy transmission line can be regarded as being composed of an infinite number of transmission line segments with a differential length of d$z$. Through each d$z$ segment, the impedance variation is d$Z(z)$. At position $z$, the impedance step change d$Z(z)$ produces a differential reflection coefficient d$D_0$:

$$\begin{aligned} \mathrm{d}D_0 &= \frac{\left[\tilde{Z}(z)+\mathrm{d}\tilde{Z}(z)\right]-\tilde{Z}(z)}{\left[\tilde{Z}(z)+\mathrm{d}\tilde{Z}(z)\right]+\tilde{Z}(z)} = \frac{\mathrm{d}\tilde{Z}(z)}{2\tilde{Z}(z)+\mathrm{d}\tilde{Z}(z)} \\ &\approx \frac{\mathrm{d}\tilde{Z}(z)}{2\tilde{Z}(z)} = \frac{1}{2}\mathrm{d}[\ln\tilde{Z}(z)] = \frac{1}{2}\frac{\mathrm{d}[\ln\tilde{Z}(z)]}{\mathrm{d}z}\mathrm{d}z \end{aligned} \quad (1)$$

If d$D_0$ is reflected at $z$=0 at the input of the gradient line, then d$D_{in}$:

$$\mathrm{d}D_{in} = \mathrm{d}D_0 e^{-\mathrm{j}2\beta z} = \frac{1}{2}e^{-\mathrm{j}2\beta z}\frac{\mathrm{d}\left[\ln\tilde{Z}(z)\right]}{\mathrm{d}z}\mathrm{d}z\,. \quad (2)$$

The total reflection coefficient $D_{in1}$ at the input of the gradient line:

$$D_{in1} = \int_0^l \mathrm{d}D_{in1} = \frac{1}{2}\int_0^l e^{-\mathrm{j}2\beta z}\frac{\mathrm{d}[\ln\tilde{Z}(z)]}{\mathrm{d}z}\mathrm{d}z\,. \quad (3)$$

The total reflection coefficient $D_{in2}$ at the input end of the wavy transmission line can be obtained:

$$\begin{aligned} D_{in2} = \int_0^l \mathrm{d}D_{in2} &= -\int_0^{2R_b} e^{-\mathrm{j}2\beta z}\sqrt{Z^2-2ZR_b}\frac{\mathrm{d}[\ln\tilde{Z}(z)]}{dz}\mathrm{d}z + \\ &\int_{2R_b}^{4R_b} e^{-\mathrm{j}2\beta z}\sqrt{Z^2-2ZR_b}\frac{\mathrm{d}[\ln\tilde{Z}(z)]}{\mathrm{d}z}\mathrm{d}z \\ &-\frac{1}{4}\int_0^{2R_b} e^{-\mathrm{j}2\beta z}\sqrt{Z^2-2ZR_b}\frac{\mathrm{d}[\ln\tilde{Z}(z)]}{\mathrm{d}z}\mathrm{d}z \\ &= -\frac{5}{4}\int_0^{2R_b} e^{-\mathrm{j}2\beta z}\sqrt{Z^2-2ZR_b}\frac{\mathrm{d}[\ln\tilde{Z}(z)]}{\mathrm{d}z}\mathrm{d}z + \\ &\int_{2R_b}^{4R_b} e^{-\mathrm{j}2\beta z}\sqrt{Z^2-2ZR_b}\frac{\mathrm{d}[\ln\tilde{Z}(z)]}{\mathrm{d}z}\mathrm{d}z \end{aligned} \quad , \quad (4)$$

where, $\sqrt{Z^2-2ZR_b}$ in the formula is the arc of the wave semicircle. As depicted in Fig. 1(b), the wavy transmission line is segmented into four semicircular arcs which are integrated over an infinitesimal length.

The magnitude of the reflection coefficient on the gradient transmission line and the wavy transmission line depends on the degree of matching between the non-uniform impedance transmission line and the characteristic impedance of the antenna. When the characteristic impedance is perfectly matched with the antenna impedance, there is minimal reflection on the transmission line, resulting in a reflection coefficient close to 0. In

this case, the signal can be efficiently transmitted to the antenna, achieving the highest transmission efficiency.

## 2 Design of the specific microstrip transmission lines

Different from the traditional quarter-wave impedance matching microstrip lines, the gradient line significantly improves antenna performance. Based on a tapered line, we designed a wavy microstrip transmission line with a non-uniform impedance distribution, which consists of periodic semicircles and offers more advantages in extending the bandwidth compared to the gradient line. The structure analysis of the gradient and wavy transmission line is depicted below.

### 2.1 Gradient transmission line

Figure 2(a) illustrates the interface model of the gradient transmission line. Figure 2(b) displays the electric field distribution of the gradient line transmission structure. Figure 2(c) clearly demonstrates the current distribution of the gradient line structure, which also exhibits a gradient trend. In the figure, $WT_1$ is connected to a transmission line with a width of $W_{12}$, and the length and width of the microstrip line are determined based on the basic theory of microstrip transmission lines. The length of *LH* is 3/4 wavelength. Keeping other parameters constant, the width of the gradient line $WT_2$ is a key parameter that affects the slope of the gradient line. As shown in Fig. 2(d), an increase in $WT_2$ results in a higher slope and a decrease in the $S_{12}$ value, indicating a decline in transmission efficiency. Figure 2(e) demonstrates the impact of $WT_2$ on the impedance of the radar antenna when loaded with the gradient transmission line. From 77 GHz to 81 GHz, as $WT_2$ increases from 0.3 mm to 0.8 mm, the real part of the antenna impedance gradually deviates from the reference line of 50 Ω, and the imaginary part of the impedance also increases, indicating a deterioration in impedance bandwidth. When $WT_2$ is 0.3 mm, the antenna exhibits a wide impedance characteristic within the range of 77-81 GHz. Figure 2(f) displays the *S* parameters of the gradient line after the final optimization with the antenna. $S_{11}$ and $S_{22}$ are basically maintained at approximately -15 dB, and the $S_{12}$ value is -0.28 dB.

### 2.2 Wavy transmission line

Figure 3(a) presents a separate model of the wavy transmission line interface. Figure 3(b) illustrates the electric field distribution of the wavy transmission line structure. Figure 3(c) illustrates that the current distribution of the wavy transmission line structure presents a wavy type. The characteristic impedance of the wavy microstrip transmission line structure changes periodically and smoothly transitions to the antenna, increasing the resonance frequency matching range of the antenna, thereby expanding the bandwidth. The transmission line at the tail of the wavy line is primarily for impedance matching with the antenna, and its width $W_b$ and length $L_b$ can be calculated. The width of the wave *LT* is the sum of the radius of the wave lobe $R_b$ and the width of the wave tail transmission line $W_b$. *LT* is significantly influenced by $R_b$, and the change in $R_b$ directly determines the transmission effect of the wave line. Therefore, an analysis is conducted on the influence of the wave radius $R_b$ on the effect of the wavy transmission line.

In Fig. 3(d), $S_{12}$ decreases regularly as $R_b$ increases. When $R_b$ is 0.1 mm, the wavy transmission line performs optimally. However, it is necessary to consider the transmission effect after connecting the antenna, and other parameters after antenna optimization are shown in Table 1.

Figure 4 illustrates the return loss optimization for the wavy transmission line. Figure 4(a) depicts $S_{11}$ curves for different values of $R_b$: 0.1 mm, 0.11 mm, and 0.12 mm. As $R_b$ increases, there is a noticeable upward shift in the $S_{11}$ curve, reflecting a change in return loss. The shift is attributed to the increase in the width of the microstrip line, which in turn raises its capacitive impedance and affects the impedance matching. Optimal performance of the wavy transmission line is observed when $R_b$ is set to 0.1 mm.

Figure 4(b) presents $S_{11}$ curves under three distinct $L_b$ conditions. Observing the figure, it is evident that an increase in $L_b$ results in an upward shift of $S_{11}$ values within the 77.5-83 GHz frequency band, while a downward shift occurs in the 83-88 GHz range. Because the length of $L_b$ increases, its impedance value will change from capacitive to inductive. Upon comprehensive analysis, it is found that when $L_b$ is set to 0.6 mm, the $S_{11}$ curve exhibits a more gradual change, which is advantageous for achieving better impedance matching with the radar antenna.

Figure 5(b) displays the *S*-parameter diagram of the final optimized single wavy transmission line. The values of $S_{11}$ and $S_{22}$ are approximately -21 dB in the 75 GHz to 88 GHz range, while the $S_{12}$ remains at -0.26 dB within its range. This also demonstrates that the energy from port 1 is effectively transmitted to port 2, with relatively low reflection coefficient and satisfactory transmission effect.

Figure 5(a) illustrates the impedance variations of the loaded wavy transmission line radar antenna under different $R_b$ conditions. Within the frequency range of 77.6-86.97 GHz, the increase of $R_b$ causes significant fluctuations in the antenna impedance. However, when $R_b$ is equal to 0.1 mm, the real and imaginary components of the antenna impedance change smoothly, with the real part approaching 50 Ω. This is because the surface current concentrates on the semi-circular segments, allowing for a wider tunability range of the resonant frequency, thereby demonstrating excellent ultra-wideband impedance characteristics. Compared with the loaded gradient line radar antenna, the wavy transmission line exhibits a significantly better extended bandwidth effect, as depicted in Fig. 6.

## 3 The millimeter wave radar antenna loaded with the gradient and wavy transmission lines

The millimeter-wave radar antenna uses Panasonic

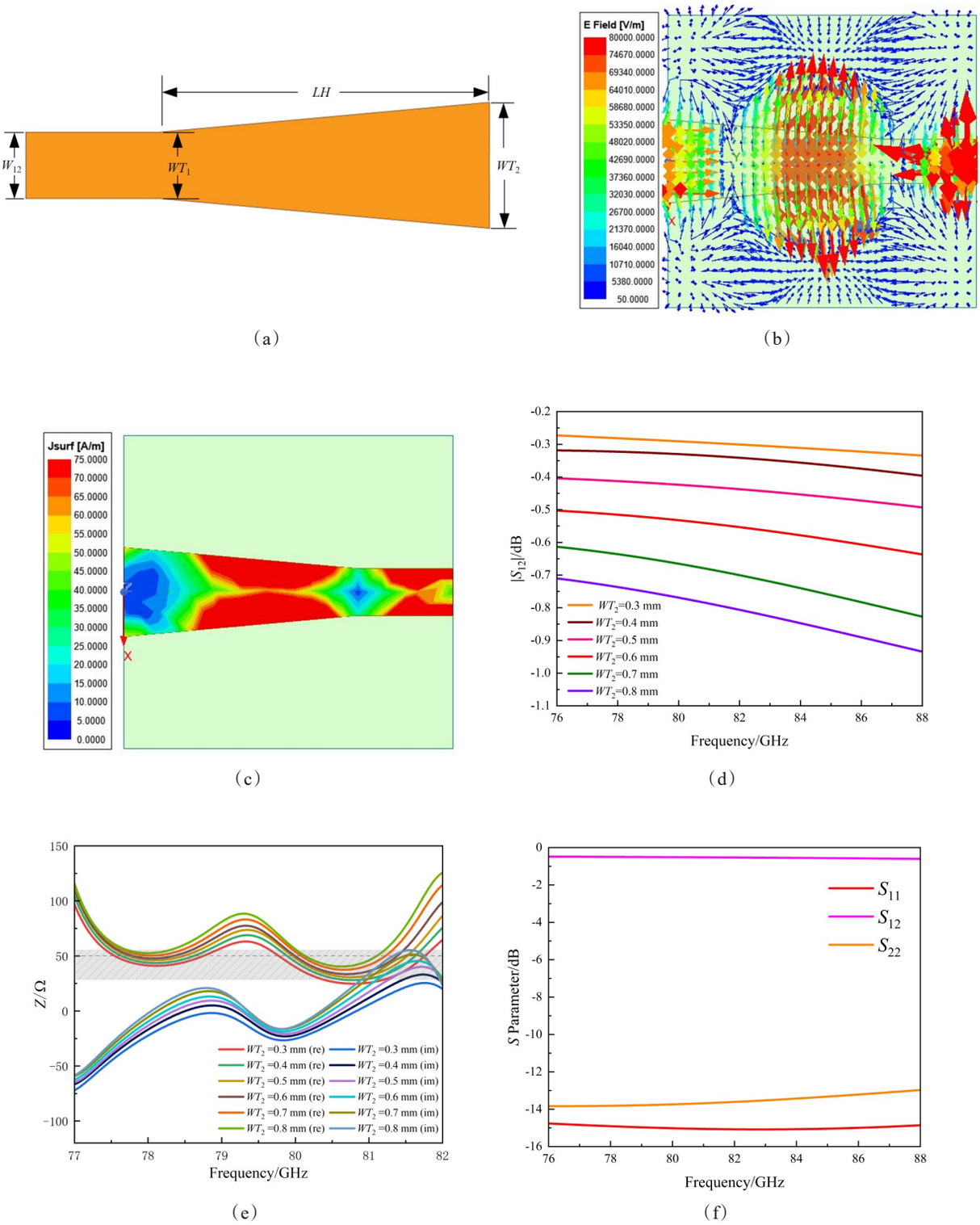


Fig. 2 Structure and performance of gradient transmission line: (a) single port model; (b) electric field vector distribution at 78 GHz; (c) surface current distribution at 78 GHz; (d) influence of $WT_2$ on the gradient transmission line; (e) influence of impedance characteristics of $WT_2$ on antenna after loading gradient transmission line; (f) transmission performance of gradient model

图2 渐变传输线的结构与性能:(a)单端口模型;(b) 78 GHz电场矢量分布;(c) 78 GHz的表面电流分布;(d) WT2对渐变传输线的影响;(e)加载渐变传输线后WT2对天线的阻抗特性变化;(f)渐变线模型的传输性能

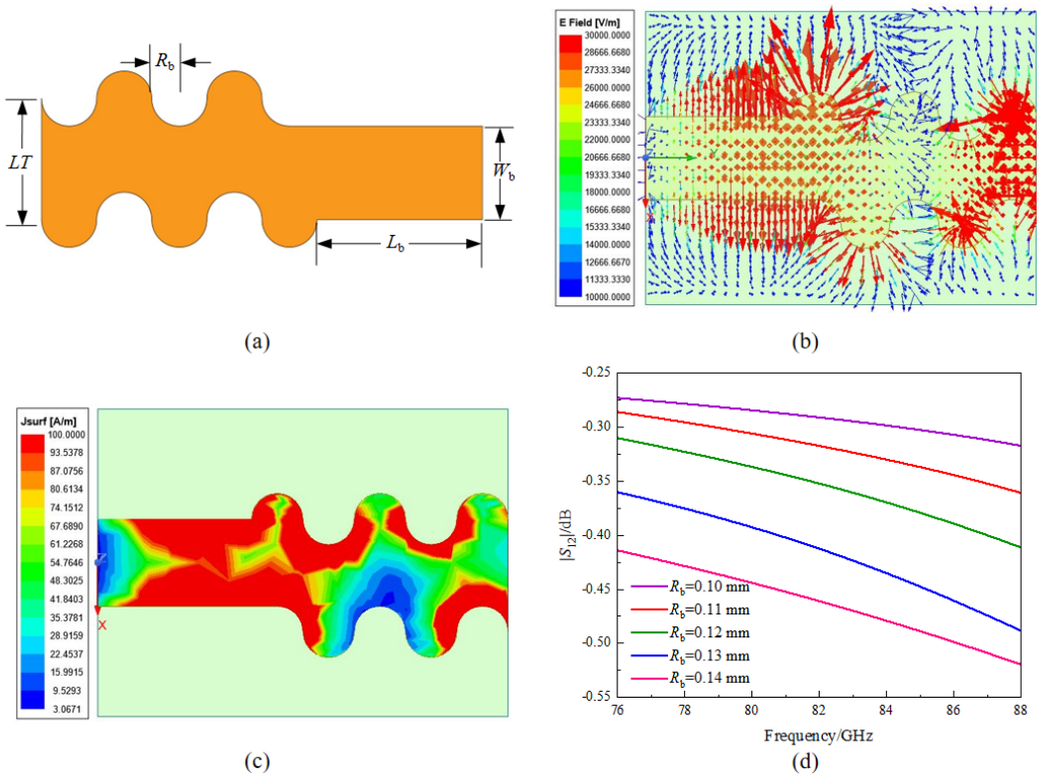


Fig. 3 Structure and performance of wavy transmission line: (a) single interface model; (b) electric field vector distribution at 78 GHz; (c) current distribution on the surface at 78 GHz; (d) effect of parameter $R_b$ on wavy transmission line
图3 波浪传输线的结构与性能:(a)单界面模型;(b) 78 GHz电场矢量分布;(c) 78 GHz表面电流分布;(d)参数$R_b$对波浪传输线的影响

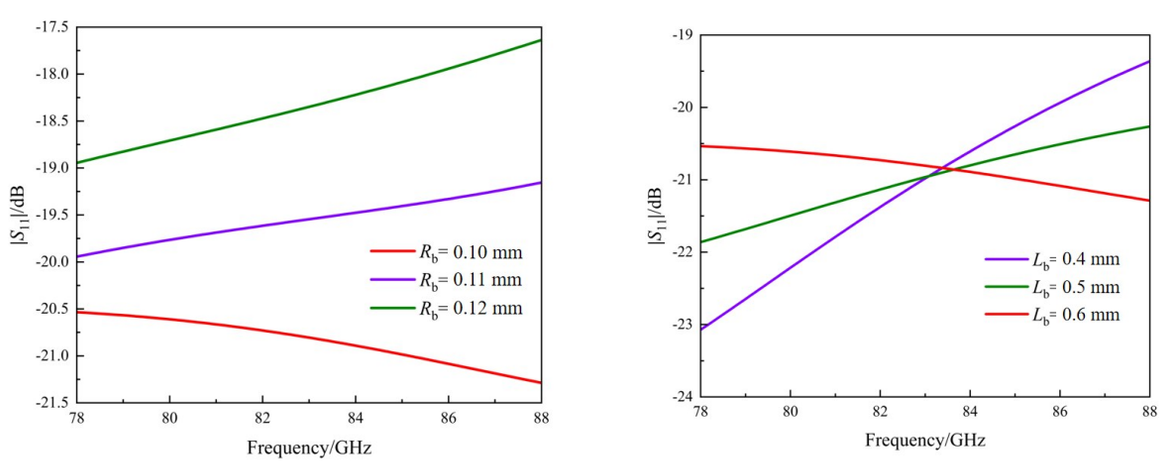


Fig. 4 Wavy transmission line return loss optimization: (a) $R_b$ ; (b) $L_b$
图4 波浪传输线回波损耗优化:(a) $R_b$;(b) $L_b$

R5515 as the dielectric substrate. The thickness of the substrate is 0.127 mm, the relative dielectric constant is 3.09, the loss tangent is 0.0035, and the thickness of the antenna patch is 0.018 mm. The wavy transmission line interface and the gradient transmission line interface are combined with the radar antenna respectively. Figure 7 shows a combined antenna model of the gradient line and wave line. In the wave antenna structure, the length of the unit radiation patch $L_j$=1.038 mm is about half of the guided wave's wavelength. In the gradient antenna structure, the length of the radiation patch is $L$=1.03 mm. The width of the radiation patch unit is tapered from the middle to both sides, and its width is $W_n$, $n$ is 1, 2, 3, 4, 5. The spacing between the radiation patches is $L_i$= 1.18 mm, and the corresponding width is $W_i$=0.1 mm. In both the wavy and the gradient transmission line anten-

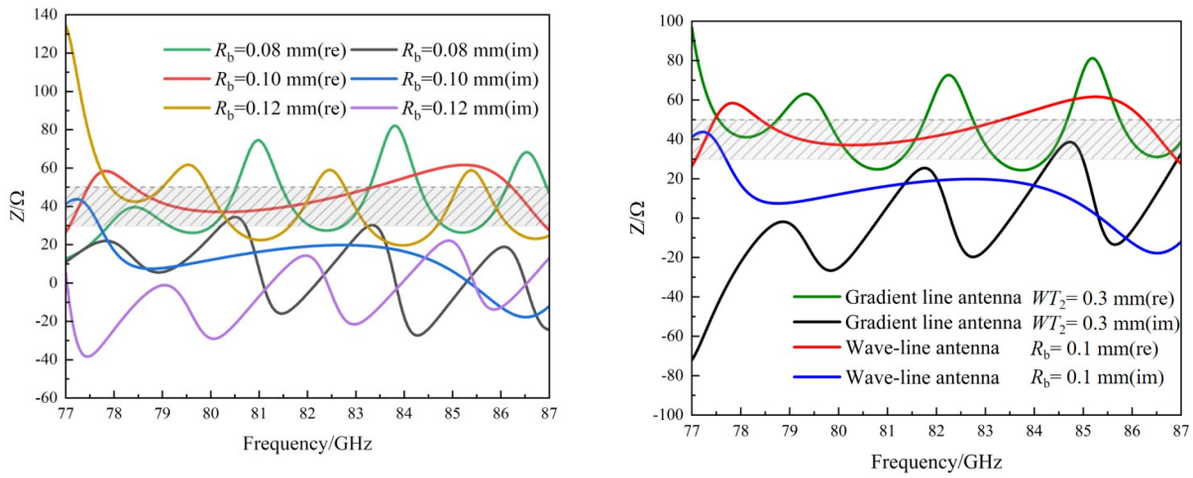


Fig. 5 Performance of wavy transmission line: (a) effect of impedance characteristics of $R_b$ on antenna after loading wavy transmission line; (b) transmission performance of wavy model

图5 波浪传输线的性能:(a) 加载波浪传输线后$R_b$对天线的阻抗特性变化;(b)波浪模型的传输性能

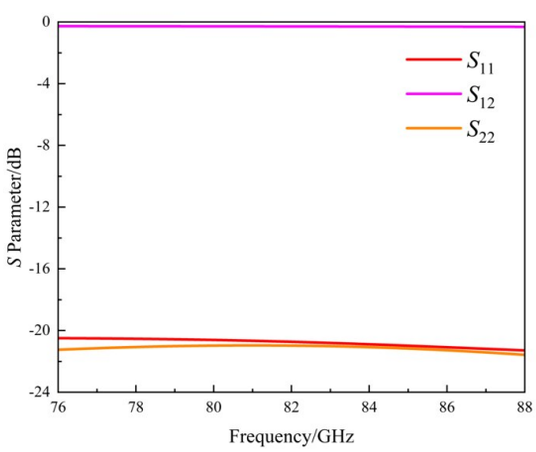


Fig. 6 Comparison of the impedance changes of the loaded wave line and the gradient line antenna, respectively

图6 分别对比加载波浪线和渐变线天线的阻抗变化

nas, the width of the unit radiation patch is consistent.

**Table 1 Parameter values of antenna (Unit/mm)**

**表1 天线的参数值(单位/mm)**

| Parameter | Value | Parameter | Value |
|---|---|---|---|
| $W_1$ | 1.34 | $L_j$ | 1.038 |
| $W_2$ | 1.195 | $L_{ji}$ | 1.18 |
| $W_3$ | 0.97 | $LH$ | 1.5 |
| $W_4$ | 0.75 | $L_b$ | 0.6 |
| $W_5$ | 0.61 | $WT_1$ | 0.3 |
| $W_{12}$ | 0.3 | $WT_2$ | 0.57 |
| $W_i$ | 0.1 | $W_b$ | 0.34 |
| $L$ | 1.03 | $L_i$ | 1.18 |
| $LT$ | 0.44 | $R_b$ | 0.1 |

The gradient length $LH$=1.5 mm of the gradient transmission line interface is 3/4 guided wave wavelength. And a microstrip matching line with a length of 1/4 wavelength is added to the front end of the gradient line, and its $W_{12}$ corresponds to the characteristic imped-

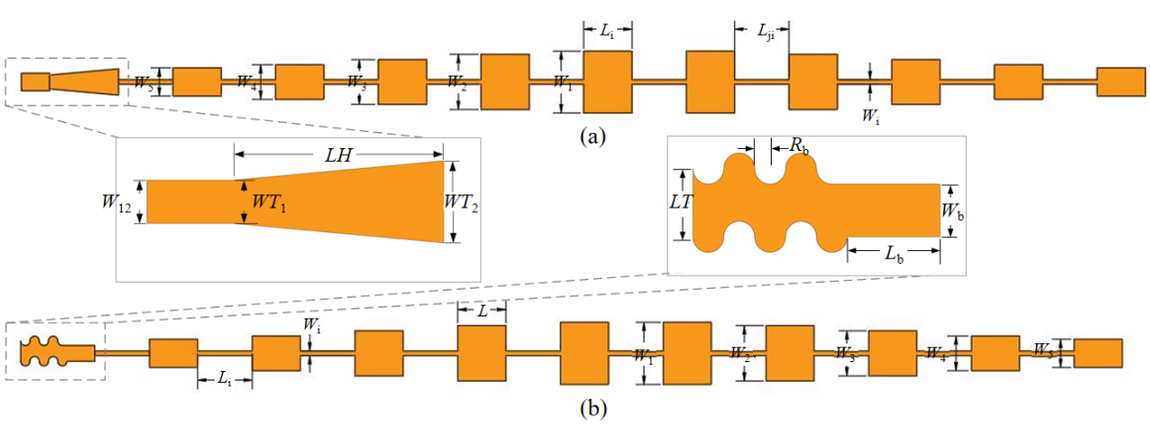


Fig. 7 Millimeter-wave radar antenna model loaded with specific transmission lines

图7 加载新型传输线的毫米波雷达天线结构

ance of 50-ohm microstrip line width at 79 GHz. A microstrip line with a length of $L_b$ and a width of $W_b$ is introduced at the contact end of the wavy transmission line and the antenna for transition. The upper and lower sides of the wavy transmission line are semi-circular waves, which change periodically and alternately along the wavy transmission line with a radius of $R_b$. *LT* is the width of the wavy transmission line, and the overall length of the wavy transmission line is about 3/4 of the guided wave wavelength. The simulation results show that the wavy transmission line antenna and the gradient transmission line antenna have high gain and bandwidth. In particular, the bandwidth effect of the wave structure is significantly improved.

Figure 8(a) shows the comparison of *S*-parameters of millimeter-wave radar antennas loaded with different transmission line matchings. Here, the bandwidth of the radar antenna loaded with the gradient line has been optimized to its maximum capacity. To explore wider bandwidth applications, the gradient line structure has been replaced with a wavy microstrip transmission line structure. Figure 8(a) shows that the $S_{11}$ value of the antenna loaded with 1/4 impedance matching is -35.84 dB at 77.69 GHz, with a working frequency band of 76.74-78.59 GHz and a bandwidth of 1.85 GHz.. However, the bandwidth needs improvement. The $S_{11}$ value of the radar antenna with gradient line reaches -34.5 dB at 78.27 GHz, with the working frequency band of 77.5-81.06 GHz and the bandwidth of 3.56 GHz. The bandwidth of the radar antenna loaded with gradient line is much wider than that of the traditional 1/4 impedance matching radar antenna. For the radar antenna with wavy transmission line, its working frequency band is 77.6-86.97 GHz, and the bandwidth is 9.37 GHz. Its working range is significantly higher than that of the gradient line.

Figure 8(b) depicts the gain fluctuation of the millimeter-wave radar antenna when loaded with both gradient and wavy transmission lines across the 77-81 GHz frequency band. Observations reveal that the gain of the antenna loaded with the wavy transmission line is marginally superior, with an average enhancement of 0.23 dB over the one loaded with the gradient. The change in gain is primarily due to the dominant influence of the radiation unit array on the radar antenna, rather than the impact of the matching transmission line.

The gain of millimeter wave radar antennas loaded with quarter-wavelength impedance matching, a gradient line structure, and a wave line are compared in Fig. 8(c). The 3 dB beam width of the radar antenna with a gradient transmission line is 9.86°, while the antenna loaded with a wavy transmission line has a 3 dB beam width of 9.58°. The beam width of the wavy transmission line radar antenna is slightly narrower than that of the gradient line radar antenna. Figure 9 shows the two-dimensional radiation patterns corresponding to the loading of the wave and gradient line radar antenna at 78 GHz, 79 GHz, and 81 GHz, respectively. It is evident that all of

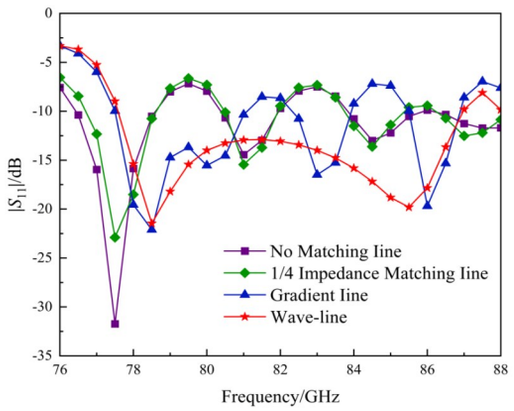


(a)

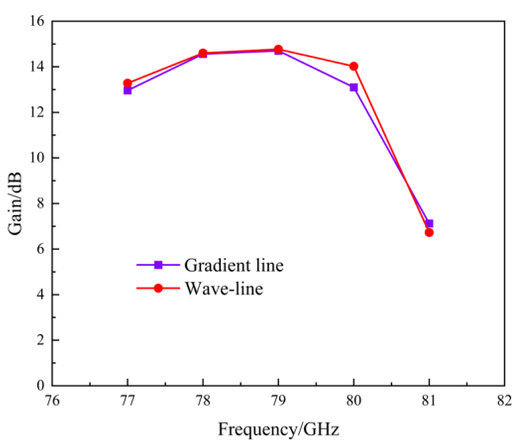


(b)

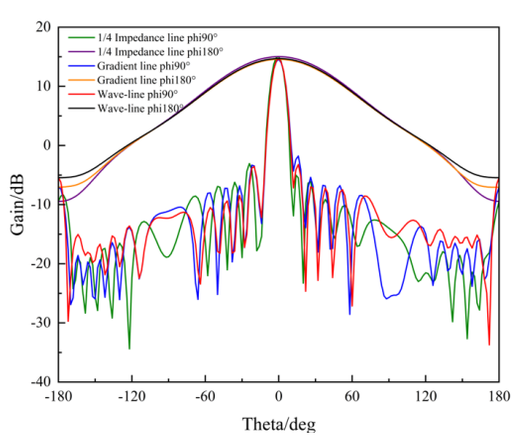


(c)

Fig. 8 Comparison of antenna performance loaded with different transmission lines: (a) comparison of *S* parameters of different transmission lines matching 1*10 linear array; (b) comparison of gain in frequency band; (c) gain of 1*10 linear array matched by different transmission lines

图8 加载不同传输线的天线性能对比:(a)不同传输线匹配1*10线阵的S参数对比;(b)频带内增益的比较;(c)不同传输线匹配的1*10线阵增益

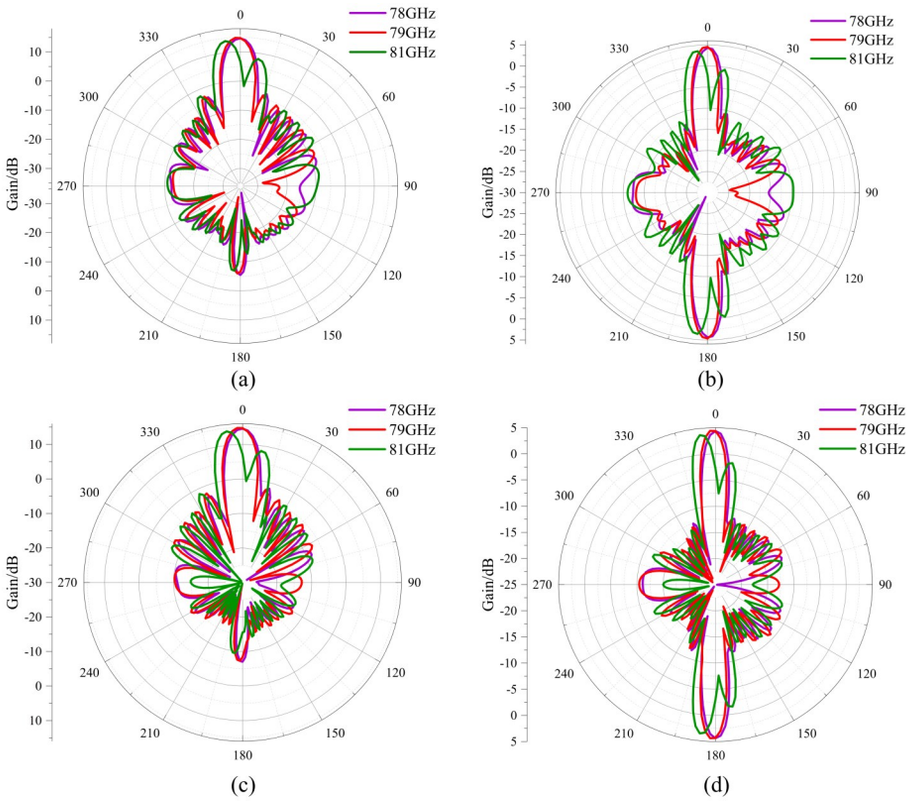


Fig. 9 Antenna pattern of wavy and gradient linear array: (a) wavy phi= 90°; (b) wavy theta= 90°; (c) gradient line phi= 90°; (d) gradient line theta= 90°
图9 波浪和渐变线阵的天线方向图:(a)波浪 Phi = 90°;(b)波浪 Theta = 90°;(c)渐变线 phi = 90°;( d )渐变线 theta = 90°

them exhibit good directivity, with the radiation energy mainly concentrated in the main lobe, resulting in better antenna radiation efficiency. Given the challenging experimental conditions, the physical object has been processed, with physical testing scheduled for the future. The prototype is illustrated in Fig. 10.

By processing the array antenna with 10 array elements, the antenna performance corresponding to the 1/4 impedance matching, gradient line, and wavy line is evaluated. Table 2 shows that the antenna loaded with a wavy transmission line structure exhibits better bandwidth performance compared to other transmission lines, making it more widely applicable. The study demonstrates that the radar antenna incorporating the wave transmission line structure not only shows good bandwidth performance but also features a simpler structure compared to previous research. Notably, the radar antenna equipped with the specific wavy transmission line structure achieves a bandwidth of 9. 37 GHz and boasts a compact size, offering convenience in processing and saving space on the plate. However, there is still room for improvement in the side lobe of the antenna.

## 4 Conclusions

In this paper, a wideband non-uniform wavy mi-

**Table 2 Performance comparison of some recent automotive radar antennas**
**表2 近年车载毫米波雷达天线的性能比较**

| | Antenna Type | Bandwidth/GHz | Gain/dB | HPBW/° | Complexity |
|---|---|---|---|---|---|
| Ref. [11] | Micro-patch | 27-28. 3 (1. 3) | 8. 55 | | simple |
| Ref. [17] | Coupe-patch | 24-25. 5 (1. 5) | 10. 85 | 11 | average |
| Ref. [18] | SIW | 75. 01-82. 12 (7. 11) | 12. 25 | 12 | complex |
| Ref. [19] | SIW-patch | 75-78. 5 (2. 5) | 18. 18 | 9 | complex |
| Ref. [20] | SIW | 75. 6-81 (4. 4) | 11. 35 | 10 | complex |
| Ref. [21] | Coupe | 77-78. 43 (1. 43) | 13. 95 | 7. 7 | average |
| Antenna only | Micro-patch | 76. 45-78. 58 (2. 13) | 14. 50 | 9. 55 | simple |
| Loaded 1/4matching | Micro-patch | 76. 74-78. 59 (1. 85) | 15. 02 | 9. 75 | simple |
| Loaded gradient line | Micro-patch | 77. 5-81. 06 (3. 56) | 14. 56 | 9. 86 | simple |
| Loaded wavy line | Micro-patch | 77. 6-86. 97 (9. 37) | 14. 69 | 9. 58 | simple |

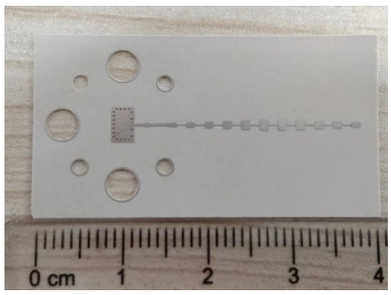


(a)

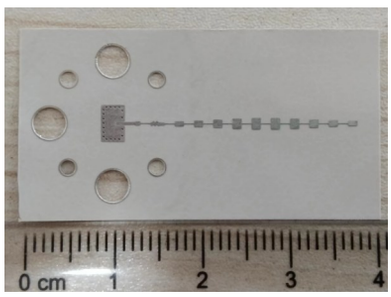


(b)

Fig. 10 Prototype of millimeter wave radar antenna: (a) gradient ;(b) wavy
图10 毫米波雷达天线实物:(a)渐变;(b)波浪

crostrip line for complex impedance at automotive radar frequency range is proposed. The non-uniform wavy transmission line is composed of periodic semi-circular segments. While the radius of the semi-circular and width of the microstrip varied, the surface current of the wave can be changed and concentrated on the semi-circular segments, so as to obtain a wider matching range of multiple resonant points, expanding the antenna radiation bandwidth. The results demonstrate that the radar antenna loaded with the wavy transmission line operates in the frequency range of 77.6-86.97 GHz and bandwidth of 9.37 GHz, which are 7.52 GHz and 5.81 GHz wider than those of the 1/4 impedance matching and the gradient lines, respectively. The gain and the half power beam width of the loaded antenna are about 14.69 dB and 9.58°, respectively. This work will have great prospects for applications in simplifying the design of vehicle-mounted millimeter-wave radar antennas, reducing associated costs, and expanding the bandwidth capabilities of traditional microstrip antennas.

## References

[1] Menzel W, Moebius A. Antenna concepts for millimeter-wave automotive radar sensors [J]. Proceedings of the IEEE, 2012, 100(7): 2372-2379.
[2] Prachi, Mandal T K. Dual frequency millimeter-wave perturbed ring patch antenna array for 5G applications [J]. IETE Journal of Research, 2023, 69(9): 5965-5974.
[3] Semkin V, Ferrero F, Bisognin A, et al. Beam switching conformal antenna array for mm-wave communications [J]. IEEE Antennas and Wireless Propagation Letters, 2015: 28-31.
[4] Al-Alem Y, Kishk A A. Efficient millimeter-wave antenna based on the exploitation of microstrip line discontinuity radiation [J]. IEEE Transactions on Antennas and Propagation, 2018, 66(6): 2844-2852.
[5] Anbarasu M, Nithiyanantham J. Performance analysis of highly efficient two-port MIMO antenna for 5G wearable applications [J]. IETE Journal of Research, 2023, 69(6): 3594-3603.
[6] Ghosh S, Sen D. An inclusive survey on array antenna design for millimeter-wave communications [J]. IEEE Access, 2019, 7: 83137-83161.
[7] Ali M M M, Patel S, HARAZ O M, et al. 8x8 millimeter-wave series-fed patch antenna array for anti-collision automotive radar [C]. 2022 IEEE International Symposium on Antennas and Propagation and USNC-URSI Radio Science Meeting (AP-S/URSI), 2022: 619-620.
[8] Lee J, Lee J M, Hwang A K C. Series feeding rectangular microstrip patch array antenna for 77 GHz automotive radar [C]. 2017 International Symposium on Antennas and Propagation (ISAP), 2017: 1-2.
[9] Yan. J, Wang. H, Yin. J, et al. Planar series-fed antenna array for 77 GHz automotive radar [C]. 2017 Sixth Asia-Pacific Conference on Antennas and Propagation (APCAP), 2017: 1-3.
[10] Yi H, Wang Z D, Xia D X, et al. Periodic asymmetric trapezoidal perturbation microstrip antenna for millimeter-wave automotive radar sensors [J]. IEEE Transactions on Antennas and Propagation, 2023, 71(2): 1369-1377.
[11] David Joseph S, Ball E A. Series-fed millimeter-wave antenna array based on microstrip line structure [J]. IEEE Open Journal of Antennas and Propagation, 2023, 4: 254-261.
[12] Yang Y-H, Sun B-H, Guo J-L. A single-layer wideband circularly polarized antenna for millimeter-wave applications [J]. IEEE Transactions on Antennas and Propagation, 2020, 68(6): 4925-4929.
[13] Afoakwa S, Jung Y-B. Wideband microstrip comb-line linear array antenna using stubbed-element technique for high sidelobe suppression [J]. IEEE Transactions on Antennas and Propagation, 2017, 65(10): 5190-5199.
[14] Lee J-H, Lee S-H, Lee H J, et al. Design of comb-line array antenna for low sidelobe level in millimeter-wave band [J]. IEEE Access, 2022, 10: 47195-47202.
[15] Lee J-H, Lee J M, Hwang K C, et al. Capacitively coupled microstrip comb-line array antennas for millimeter-wave applications [J]. IEEE Antennas and Wireless Propagation Letters, 2020, 19(8): 1336-1339.
[16] Lee J-I, Lee J-H, Lee S-H, et al. Low sidelobe design of microstrip comb-line array antenna using deformed radiating elements in the millimeter-wave band [J]. IEEE Transactions on Antennas and Propagation, 2022, 70(10): 9930-9935.
[17] De Cos Gomez M E, Fernandez Alvarez H, Florez Berdasco A, et al. Compact wearable antenna with metasurface formMillimeter-wave radar applications [J]. Materials (Basel), 2023, 16(7): 2553-2571.
[18] Teng X, Ma K, Yan N, et al. A low-cost antenna using SISL technology with suppressed sidelobe level for 77 GHz automotive radar [J]. IEEE Antennas and Wireless Propagation Letters, 2022, 21(9): 1832-1836.
[19] Jun Xu, Wei Hong, Hui Zhang, et al. Design and measurement of array antennas for 77GHz automotive radar application [C]. 10th UK-Eur-China Workshop Millimeter Waves THz Technol (UCMMT), 2017: 1-4.
[20] Teng X, Luo Y, Yann N, et al. A cavity-backed antenna using SISL technology for 77 GHz band application [J]. IEEE Transactions on Antennas and Propagation, 2022, 70(5): 3840-3845.
[21] Zeng T-X, Jiang X, Chen K-L. 77 GHz high gain antenna based on microstrip coupling excitation [C]. 2023 International Conference on Microwave and Millimeter Wave Technology (ICMMT), 2023: 1-3.